Available online at www.sciencedirect.com
ScienceDirect
Earth and Planetary Science Letters 256 (2007) 567–576
EPSL
www.elsevier.com/locate/epsl

How much potassium is in the Earth's core? New insights from partitioning experiments

Alexandre Corgne [a,b,*], Shantanu Keshav [a,1], Yingwei Fei [a], William F. McDonough [c]

[a] Geophysical Laboratory, Carnegie Institution of Washington, Washington, DC 20015, USA
[b] GEMOC, Macquarie University, North Ryde, NSW, 2109, Australia
[c] Department of Geology, University of Maryland, College Park, MD 20742, USA

Received 6 November 2006; received in revised form 31 January 2007; accepted 2 February 2007
Available online 13 February 2007
Editor: R.W. Carlson

Abstract

The presence of potassium in the core is a vexing issue in Earth Science that is of fundamental concern to the energy budget of the Earth. New experimental data reported here for partitioning of potassium (K) between peridotitic silicate melt and Fe–Ni–S–C–O molten alloy at 1650–2200 °C and 1.0–7.7 GPa reveal a negligible effect of pressure on K partitioning, at least up to 7.7 GPa. No evidence for a systematic increase of K solubility in the alloy with temperature or pressure and S or C contents in the alloy was found. However, there is a possible increase in the K partition coefficient with increasing O content in the molten alloy. Our results, which are appropriate to model core formation in a shallow magma ocean, suggest it is unlikely to sequester more than a few tens of ppm of K into Earth's core during a magma ocean event if oxygen is not a major contributor to the light element budget of the core.
© 2007 Elsevier B.V. All rights reserved.

Keywords: potassium; geodynamo; Earth's core; high pressure; metal–silicate partitioning

1. Introduction

The inner dynamics of the Earth depend largely on the energy budget of its core. Crystallization of the inner core, generation of the magnetic field and convection in the outer core and mantle are intimately linked to the amount of heat present in the core. In addition to primordial heat, the latent heat of crystallization of the inner core and the gravitational energy associated with the exclusion of light element component(s) from the solid inner core are energy sources thought to contribute significantly to the core heat budget [1,2]. Another possible source may come from the radioactive decay of long-lived radionuclides (e.g. K, U and Th) that are potentially present in the core. In the absence of radioactive heating, predicted high rates of core-mantle heat flow (6–15 TW) are consistent with an inner core age of less than ~2.5 Ga (e.g. [3–5]). However, accurately describing the heat budget of the core depends on an accurate determination of the amount

* Corresponding author. GEMOC, Macquarie University, North Ryde, NSW, 2109, Australia. Tel.: +61 29850 8258; fax: +61 2 9850 6904.
E-mail addresses: acorgne@els.mq.edu.au (A. Corgne), keshav@uni-bayreuth.de (S. Keshav), fei@gl.ciw.edu (Y. Fei), mcdonoug@geol.umd.edu (W.F. McDonough).
[1] Present address: Bayerisches Geoinstitut, Universität Bayreuth, D-95440, Bayreuth, Germany.

0012-821X/$ - see front matter © 2007 Elsevier B.V. All rights reserved.
doi:10.1016/j.epsl.2007.02.012

of heat-producing elements present in the core and on accurate estimate of the core's ohmic dissipation (loss due to electrical resistance), for which recent estimates give a wide range of values [2–6]. Both the presence of heat-producing elements in the core and a lower ohmic dissipation would permit slower rates of cooling and inner core growth [2,4]. The purpose of this contribution is to provide insights into the amount of radioactive heating in the core.

K, U and Th are generally considered lithophile and are not predicted to have an affinity for core forming materials. U and Th have estimated concentrations, absolute and relative, in the bulk silicate Earth (BSE) that are consistent with the chemical budget of the Earth if it is assumed to be of chondritic composition (e.g. [7]). This estimate leaves little room for U and Th in the core. In contrast to U and Th, K is depleted in the silicate Earth relative to CI-chondrite by about 50% (Fig. 1). This has been generally interpreted as a result of significant volatilization in the solar nebula prior to Earth's accretion (e.g. [10]). This argument has also been proposed to explain the depletion of Li, B, Na, Rb, F, Zn, Ga and to some extent Mn, Cr and V. As shown in Fig. 1, most of these elements plot on a single trend, known as the volatility trend. Interestingly, V, Cr, and Mn depletions are stronger than for the other 'volatile' elements. This secondary depletion feature is consistent with their presence in Earth's core assuming core-mantle differentiation in a deep magma ocean since these elements become siderophile at high-temperatures [11,12]. One should ask the question whether K, which plots on the low side of the volatility trend, becomes siderophile or chalcophile (assuming S is present in the core) at high-temperatures and/or high-pressures.

The presence of K in Earth's metallic core as a significant radioactive energy source was suggested over three decades ago (e.g. [13]). Despite numerous theoretical and experimental studies, it is not clear whether K is present in the core and contributes by radioactive decay to the energy budget of Earth's geodynamo. Quantum mechanics calculations [14] show that the electronic structure of potassium changes from 4s- to 3d-like orbital bonding between 20–30 GPa. If this change takes place, potassium would behave like a transition metal at high pressure, and hence its solubility in liquid alloy should increase. The effect of pressure on potassium solubility has remained uncertain, however. Shock experiments on $KFeS_2$ [15] and molecular orbital calculations assuming high-pressure conditions [16] provide arguments against the presence of potassium in planetary cores, whereas diamond anvil experiments shows potassium alloying with nickel and

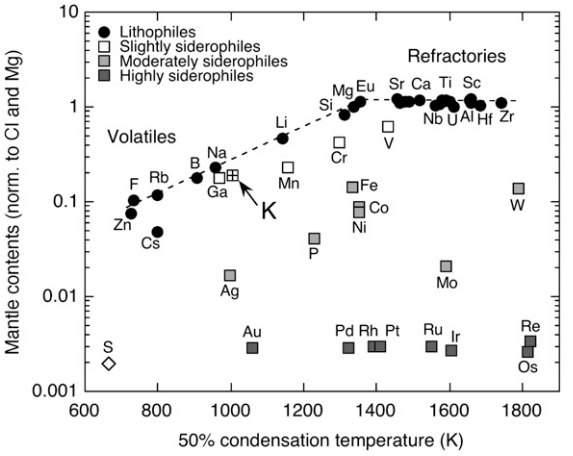

Fig. 1. Elemental abundances in the silicate Earth normalized to CI carbonaceous chondrite and Mg plotted relative to 50% condensation temperature at 10^{-4} atm pressure, which is used as a proxy for a nebular condensation sequence. Data for condensation temperatures and CI chondrite composition are from Lodders [8] and data for composition of the silicate Earth are from McDonough [9]. Note the slightly lower position of K relative to the volatility trend.

iron at ~30 GPa and ~2200 °C [17,18]. Previous experimental studies on K partitioning between metal and silicate liquids provide contradictory results concerning the fate of potassium during the favoured scenario of core formation in a silicate magma ocean, because of experimental and analytical artefacts, large extrapolation to higher pressures and temperatures, and use of oversimplified chemical compositions for study (e.g. [19–24]). Here, we report results of silicate melt-liquid alloy partitioning experiments of K to 2200 °C and 7.7 GPa (equivalent to a ~250 km deep magma ocean) on a model CI-chondrite composition relevant to model bulk Earth's differentiation. These data also allow us to re-examine the effects of pressure, temperature and alloy composition on K partitioning. Given the possibility of change in electronic structure at ~30 GPa [14,17,18] and core-mantle equilibration at significantly higher depths than the one investigated in this study (e.g. [25–28]) we caution the reader that our results may be only applicable to core segregation in a magma ocean less than about 800 km deep.

2. Experimental and analytical methods

At ambient and moderate pressures, it is known that potassium is not soluble in a pure Fe metallic liquid. All previous experiments were focused on potassium partitioning between Fe–S liquids and silicate melts on the basis that K_2S is soluble in Fe–S liquids. In

contrast to previous studies, which used compositions with high S and K contents, we used as starting material a CI-chondrite model composition containing moderate amounts of S and K, 1.9 wt.% and 4.7 wt.% respectively (Table 1). The S amount of 1.9 wt.% should be seen as an upper bound for a bulk Earth content, since it is about 3 times recent estimates of cosmochemical abundance (e.g. [9,29,30]). The potassium bulk content was chosen to ensure contents in the alloy above detection limits of the electron microprobe. The starting composition was prepared from high-purity powdered oxides (SiO_2, Al_2O_3, Fe_2O_3, MgO), carbonates (K_2CO_3, $CaCO_3$), and metal (Fe, Ni, FeS). Following the work of Thibault and Walter [31], the proportions of SiO_2, Al_2O_3, MgO, CaO, Fe and Ni were chosen to be that of model CI chondrite [32]. 1.9 wt.% of S was added to the mixture as FeS. The relative abundance of metal Fe and Fe_2O_3 is such that, after melting, the amount of FeO in the silicate melt is close to the primitive mantle value. First, the required proportions of dried SiO_2, Al_2O_3, MgO, CaO (as $CaCO_3$) and K_2O (as K_2CO_3) were mixed, then slowly decarbonated in air from 600 to 1000 °C. The appropriate amounts of Fe_2O_3, Fe, FeS and Ni were then added. The starting powder was mixed and ground under ethanol to ensure homogeneity, finally dried at 100 °C for 24 h, and stored in a desiccator to minimize water content.

Melting experiments were performed at 1650–2200 °C and 1.0–7.7 GPa, using an end-loaded, piston-cylinder apparatus and a 1500-ton multi-anvil press at the Geophysical Laboratory. Piston-cylinder experiments were conducted at 1.0 GPa using half-inch talc-pyrex pressure cells with straight graphite furnace and magnesia spacers. Temperature was monitored by a WRe5%–WRe26% thermocouple inserted axially in an alumina sleeve above the capsule. A pressure correction of 10% to the nominal pressure was applied to account for frictional losses. Multi-anvil experiments were carried out at 3.6 and 7.7 GPa in 18 mm edge length, cast, finned octahedra made of an MgO-based ceramic (Ceramacast 584, Aremco Products, Inc.), which were contained within Kennametal tungsten carbide cubic anvils with 11 mm truncated edge length. Outer zirconia sleeves were used as thermal insulator. Inside the straight graphite heater, a magnesia sleeve and alumina spacers surrounded the sample capsule made of high-purity graphite. To assess the potential influence of K loss during experiments on K partitioning, double Mo–C and Pt–C capsules were also used. Temperature was monitored by a WRe5%–WRe26% thermocouple inserted axially ~0.5 mm above the sample chamber. For this type of 18/11 assembly, Van Westrenen et al. [33] estimated the axial length of the hot spot region to be virtually independent of run temperature and on the order of ~3 mm, temperature variation within the hot spot region being less than 20 °C. No correction to account for axial temperature gradient was made to the thermocouple readings. Radial temperature gradient from the centre

Table 1
Experimental conditions and run products

Run	*P* (GPa)	*T* (°C)	*t* (s)	Capsule	Products and proportions	ΔIW	NBO/T	K loss (%)
PC509	1.0	1700	120	C	Sil (78)+Spa (17)+Sul (5)	−1.9	2.7	14
PC504	1.0	1650	100	Pt–C	Sil (76)+Spa (19)+Sul (5)	−1.9	2.7	17
PC508	1.0	1700	300	Pt–C	Sil (77)+Spa (18)+Sul (5)	−1.9	2.6	13
PC514	1.0	1840	20	Mo–C	Sil (79)+Spa (15)+Sul (6)	−1.7	2.8	14
PC515	1.0	1900	100	Mo–C	Sil (77)+Spa (18)+Sul (5)	−1.9	2.6	15
PR380	3.6	1800	100	C	Sil (77)+Spa (18)+Sul (5)	−2.0	2.7	22
PR381	3.6	2000	100	C	Sil (74)+Spa (20)+Sul (6)	−2.1	3.0	44
PR382	3.6	2200	100	C	Sil (74)+Spa (21)+Sul (5)	−2.0	2.6	40
PR390	3.6	1850	180	Mo–C	Sil (76)+Spa (18)+Sul (6)	−2.0	2.6	16
PR394	3.6	2000	100	Mo–C	Sil (76)+Spa (19)+Sul (5)	−2.0	2.6	17
PR395	3.6	2150	100	Mo–C	Sil (76)+Spa (19)+Sul (5)	−1.9	2.8	24
PR377	7.7	2000	100	C	Sil (75)+Spa (25)	−2.0	2.6	16
PR378	7.7	2200	100	C	Sil (75)+Spa (25)	−2.0	2.7	9
PL191	7.7	2100	100	Mo–C	Sil (77)+Spa (23)	−1.9	2.6	11
PR396	7.7	2025	100	Mo–C	Sil (77)+Spa (23)	−1.9	2.6	12

Abbreviations are: *P*, pressure; *T*, temperature; *t*, duration; Sil, silicate melt; Spa, S-poor alloy; Sul, sulphide; ΔIW, relative log fo_2 below the iron-wüstite oxygen buffer; NBO/T, molar ratio of non-bridging oxygens to tetrahedral cations in the silicate melt calculated assuming all Fe as Fe^{2+} and ignoring the effect of S. Oxygen fugacity (ΔIW) was calculated from the Fe content of the S-poor alloy and FeO content of the silicate melt assuming ideal mixing behaviour. Modal proportions of the run products were determined by least-square mass balance calculation of major elements (Fe, Mg, Si, S, O).

position is estimated to be ~25 °C/mm [33]. From these results and given the size of the sample chamber (∅ ~400 μm, L ~500 μm) and its position at the centre of the assembly, the temperature variations within the sample are expected to be on the order of 10 °C. No pressure correction was made to the thermocouple electromotive force. For the 18/11 assembly, pressure was calibrated using the quartz/coesite transition at 3.2 GPa and 1200 °C [34], fayalite/spinel transition in Fe_2SiO_4 at 5.75 GPa and 1200 °C [35], garnet/perovskite transition in $CaGeO_3$ at 5.9 GPa and 1200 °C [36], and coesite/stishovite transition at 8.7 GPa and 1000 °C and 9.2 GPa and 1200 °C [37]. Pressure uncertainty is estimated to be ±0.2 GPa at 3.6 GPa and ±0.3 GPa at 7.7 GPa based on the width of the brackets for the different transitions investigated. Temperature effects on pressure calibration were assumed to be negligible. The samples were pressurized at room temperature, then raised at 150 °C/min to 1500 °C, and at 250 °C/min to the target temperature and held there for 20–300 s. Temperature was maintained to within ±3 °C of the set point with a programmable controller connected to the thermocouple and thyristor. The samples were quenched at an estimated rate of 500 °C/s by switching off the power to the furnace and then gradually decompressed. As done in previous metal-silicate partitioning studies (e.g. [31]), we kept run durations relatively short to minimize metal infiltration into the C capsules resulting from surface-energy characteristics between metal liquid, silicate melt, and capsule. Furthermore, Thibault and Walter [31] have shown that run durations as short as a few tens of seconds were sufficient to approach chemical equilibrium in this type of experiments. We were unable to collect partitioning data from multi-anvil runs performed at pressures above 7.7. GPa. As observed by Thibault and Walter [31], capsule transformation to diamond at these conditions induced rapid liquid metal dispersion within the capsule. Experimental conditions and products of successful runs are reported in Table 1.

Recovered capsules were mounted into epoxy resin which was hardened overnight at ~40 °C (not at the common temperature of ~100 °C to minimize K loss). It has been recognized that polishing of an experimental run product containing K for chemical analysis using water or oil lubricants results in substantial K loss from the metallic phase (e.g. [23]). Therefore, run products were polished dry using silicon carbide abrasive sheets (240–600 grit) and diamond-coated films (1–12 μm). A good polish was obtained down to 3 μm. In contrast to Murthy et al. [23], we did not use boron nitride as lubricant during the lapping operation because it tends to stick to the sample surface. Major and minor element contents of the experimental charges were measured using the 5-spectrometer JEOL 8900 electron microprobe at the Geophysical Laboratory and the 5-spectrometer Cameca SX100 at GEMOC. A beam current of 15 nA and an accelerating voltage of 15 kV were used to minimize K volatilization during analysis. Repetitive analyses of the same sample spot do not show evidence for K volatilization with current up to 15 nA. As calibration standards, we used orthoclase to measure K content and a series of silicates (basalt, kyanite, olivine, wollastonite, diopside, andradite), oxides ($MgCr_2O_4$, $BaSO_4$), metal (Ni) and sulphides (pyrite, chalcopyrite) to measure the remaining elements. Counting times ($Elt_{Pk/Bg}$) were: (1) for the alloy phase: $Si_{60/30}$, $Al_{60/30}$, $Mg_{60/30}$, $Ca_{100/50}$, $Fe_{30/15}$, $S_{60/30}$, $K_{200/100}$, $Ni_{30/15}$ and $O_{200/100}$; (2) for the silicate melt: $Si_{30/15}$, $Al_{30/15}$, $Fe_{30/15}$, $Ca_{30/15}$, $K_{60/30}$, $Mg_{30/15}$, $Ni_{60/30}$ and $S_{60/30}$. Analyses were made with a defocused beam of 30 μm diameter for the silicate phase and of 5–10 μm diameter for the alloy to minimize K volatilization and average the compositions of the fine-grained quench phases that composed alloy and silicate phases. With this setup, typical detection limits (3σ) were: (1) for the liquid alloy: 70 ppm for K, 110 ppm for Mg, 150 ppm for Si, Al, S and Ca, 360 ppm for O, and 600 ppm for Ni and Fe; (2) for the silicate melt: 120 ppm for S, 180 ppm for K, Al and Ca, 240 ppm for Si and Mg, 280 ppm for Ni, and 370 ppm for Fe. For analytical operating conditions of 25 kV and 300 nA, Chabot and Drake [21] found that secondary fluorescence from the neighbouring silicate phase interfered with measurements of the alloy composition if measurements were made within 50 μm of the silicate phase. For the operating conditions of this study, measurement of the alloy composition can be carried out closer to the alloy-silicate interface. Using measured contents of Si, Al, Ca and Mg as indicator of silicate contamination, we did not observe any systematic secondary fluorescence for both sulphide and S-poor alloy. Near-edge analyses that revealed contents for these elements above detection limits were discarded.

3. Results and discussion

3.1. Phase relations and composition

All samples contain several quench blebs of molten alloy up to ~200 μm across and surrounded by quench silicate melt, the latter constituting 76±2 wt.% of the experimental charge (Table 1). In agreement with the recent experimental work of Urakawa et al. [38] and Tsuno et al. [39], we observe immiscibility between sulphide (~30 wt.% S) and S-poor alloy (0.6–1.5 wt.%

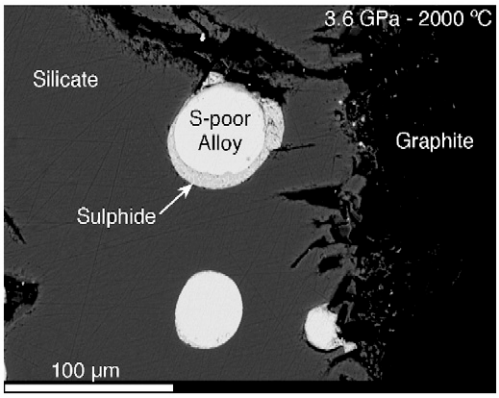

Fig. 2. Back-scattered electron image of the products of run PR394 showing typical phase morphologies and dimensions at 1.0 and 3.6 GPa. At 7.7 GPa, there is a complete miscibility between sulphide and S-poor alloy.

S) at 1.0 and 3.6 GPa. The sulphide phase (~5% of the total weight) is usually present at the interface between silicate melt and S-poor alloy as a 10–20 µm thick layer. At 7.7 GPa, there is complete miscibility and the molten alloy contains ~7 wt.% S. A back-scattered electron image of typical run products is presented in Fig. 2. Compositions of the silicate melt and liquid alloys and K partition coefficients (D_K, the weight ratio of K content in liquid alloy over K content in silicate melt) are given in Table 2. Because of its small size and larger grain quench texture, the sulphide phase was the most difficult to analyse. This led to relatively large uncertainties on the sulphide composition (Table 2).

Electron microprobe profiles across the alloy and silicate phases suggest that phases are compositionally homogeneous, hence that equilibrium conditions were approached. Within uncertainties, the sulphide contains approximately the same amount of Ni (~5 wt.%) as the S-poor alloy (Table 2). Its oxygen content is notably higher, however, between 0.5 and 1.5 wt.%, as opposed to ~0.2 wt.% for the S-poor alloy (Table 2). By difference, we estimate the carbon content to be lower in the sulphide phase (~1–4 wt.%) than in the coexisting S-poor alloy phase (5–7 wt.%). After closure of the immiscibility gap at 7.7 GPa, the C alloy content is intermediate on the order of 4–5 wt.%. The potassium contents in the metal alloy are above detection limits and vary between 250 and 1150 ppm, with higher contents for the sulphide phase (Table 2). Silicate melts are peridotitic in composition, with NBO/T of ~2.7 (Table1), ~12 wt.% FeO and ~6 wt.% K_2O (Table 2). Oxygen fugacity in our runs was calculated from the composition of coexisting S-poor alloy and silicate assuming ideal mixing. Results show that silicate and alloy equilibrated at approximately 2 log units below the iron-wüstite buffer, which represents the average oxygen fugacity for mantle-core equilibration.

3.2. Effect of temperature and pressure on K partitioning

Pressure and temperature can have significant influence on element partitioning between silicate melt and liquid alloy. This has been well documented for Ni, Co, and other moderately siderophile elements (e.g. [31]). In agreement with previous studies (e.g. [40]), we find that D_S for both S-poor alloy and sulphide increases with increasing pressure but decreases with increasing temperature. In contrast, the D_O trend is opposite to that for D_S, a result consistent with the experimental work of Rubie et al. [41]. Potassium partition coefficients are plotted as a function of temperature in Fig. 3. In agreement with previous studies [21,22,24] we find that K is more incompatible in S-poor alloy (Fig. 3a) than in sulphide (Fig. 3b). As we will discuss in Section 3.3, this difference is related to compositional effect. Looking separately at sulphide and S-poor alloy, the combined effect of pressure and temperature appears negligible. D_K values remain identical within uncertainty over the range of pressure and temperature conditions of this study, with D_K of 0.007±0.003 for S-poor alloy and 0.017±0.006 for sulphide (Table 2). Our results for sulphide are in good agreement with the data point of Murthy et al. [23] at 2 GPa and 1800 °C. However, as shown in Fig. 3, our results are in marked contrast with the predictions of Murthy et al. [23]. These authors showed that K enters sulphide liquid coexisting with polymerized silicate melt (NBO/T<1) with a strong dependence on temperature, but without a significant dependence on pressure over their range of study (1–3 GPa). More recently, Bouhifd et al. [24] reached similar conclusions using new experimental results together with a compilation of previously published partitioning data. Although our results agree that there is not a strong pressure dependence on D_K at least up to ~8 GPa, we find no evidence for an increase of D_K with increasing temperature. Murthy et al. [23] and Bouhifd et al. [24] extrapolated their data to conditions of temperature and melt structure appropriate to core segregation in a deep magma ocean (40±20 GPa and 3200±500 °C average P–T conditions) and concluded that K is a substantial radioactive heat source in S-bearing planetary cores. One critical issue in the reasoning followed by Murthy et al. [23] and Bouhifd et al. [24] is the assumption that the temperature dependence obtained for simple compositional system is identical for more appropriate alloy and silicate compositions as the ones of

this study. Our data demonstrate that this assumption is not valid for both S-poor alloy and sulphide. In the absence of temperature and pressure effect on K partitioning, as our data indicate, the partition coefficients for K remain too low to allow significant amounts of K to enter core materials segregating in the putative magma ocean. However, as we discuss below, compositional factors must also be taken into account to determine appropriate D_K values.

3.3. Compositional control: sulphur, carbon or oxygen?

As mentioned above, K is more incompatible in S-poor alloy than in sulphide (Fig. 3), implying that an increase of

Table 2
Composition (in wt.%) of starting material and run products and K partition coefficients

	Phase	Si	Al	Mg	Ca	Fe	Ni	S	K	O	Total [a]	D_K
CI-model		15.78	1.29	14.56	1.39	27.41	1.51	1.89	4.70	31.47	100.00	
PC509	Sil (n=15) [b]	20.19 (5) [c]	1.60 (2)	18.72 (22)	1.73 (4)	10.08 (10)	<DL	0.39 (2)	5.19 (11)	41.71 (28)	99.62	
	Spa (n=22)	<DL [d]	<DL	<DL	<DL	87.27 (59)	5.64 (21)	0.62 (20)	0.025 (6)	0.18 (2)	93.74	0.0047 (11)
	Sul (n=5)	<DL	<DL	<DL	<DL	61.27 (80)	4.97 (199)	30.17 (239)	0.095 (49)	0.74 (19)	97.25	0.018 (9)
PC504	Sil (n=22)	20.22 (62)	1.59 (7)	18.97 (55)	1.70 (8)	10.66 (21)	<DL	0.27 (2)	5.11 (23)	41.92 (62)	100.43	
	Spa (n=16)	<DL	<DL	<DL	<DL	86.09 (21)	6.18 (6)	0.80 (7)	0.036 (10)	0.16 (1)	93.27	0.0070 (19)
	Sul (n=7)	<DL	<DL	<DL	<DL	60.63 (240)	4.17 (204)	30.22 (426)	0.075 (26)	0.69 (33)	95.78	0.015 (5)
PC508	Sil (n=25)	20.35 (7)	1.72 (7)	18.72 (54)	1.78 (8)	10.45 (18)	<DL	0.37 (3)	5.30 (25)	42.13 (64)	100.83	
	Spa (n=34)	<DL	<DL	<DL	<DL	87.59 (17)	5.43 (10)	1.11 (10)	0.029 (5)	0.17 (1)	94.34	0.0055 (9)
	Sul (n=7)	<DL	<DL	<DL	<DL	60.31 (201)	5.32 (268)	30.57 (399)	0.057 (16)	0.82 (34)	97.07	0.011 (3)
PC514	Sil (n=25)	19.43 (6)	1.58 (6)	17.74 (45)	1.70 (6)	12.66 (17)	<DL	0.36 (2)	5.11 (22)	40.87 (53)	99.45	
	Spa (n=16)	<DL	<DL	<DL	<DL	86.95 (25)	6.20 (23)	0.66 (12)	0.032 (6)	0.17 (1)	94.01	0.0062 (12)
	Sul (n=4)	<DL	<DL	<DL	<DL	61.17 (199)	7.90 (3)	26.63 (285)	0.115 (39)	1.23 (33)	97.05	0.023 (8)
PC515	Sil (n=18)	20.01 (6)	1.68 (6)	18.03 (47)	1.75 (5)	10.60 (9)	<DL	0.33 (2)	5.18 (19)	41.22 (52)	98.79	
	Spa (n=14)	<DL	<DL	<DL	<DL	87.08 (78)	5.22 (10)	0.68 (11)	0.046 (9)	0.21 (1)	93.23	0.0089 (19)
	Sul (n=6)	<DL	<DL	<DL	<DL	60.78 (70)	3.53 (253)	32.78 (265)	0.064 (11)	0.65 (22)	97.81	0.012 (2)
PR380	Sil (n=51)	20.14 (3)	1.40 (2)	19.60 (19)	1.65 (2)	8.99 (4)	<DL	0.14 (1)	4.73 (9)	41.38 (20)	98.03	
	Spa (n=22)	<DL	<DL	<DL	<DL	88.44 (39)	4.87 (6)	1.34 (19)	0.038 (3)	0.19 (5)	94.88	0.0080 (7)
	Sul (n=4)	<DL	<DL	<DL	<DL	62.59 (82)	6.30 (196)	29.15 (2.51)	0.076 (28)	0.49 (11)	98.60	0.016 (6)
PR381	Sil (n=42)	19.89 (8)	1.20 (4)	21.68 (29)	1.81 (6)	8.75 (20)	<DL	0.21 (2)	3.54 (12)	42.12 (42)	99.20	
	Spa (n=15)	<DL	<DL	<DL	<DL	87.29 (52)	4.82 (29)	1.26 (10)	0.034 (11)	0.21 (2)	93.61	0.0096 (31)
	Sul (n=7)	<DL	<DL	<DL	<DL	62.47 (168)	7.82 (282)	24.32 (325)	0.040 (20)	0.87 (29)	95.51	0.011(6)
PR382	Sil (n=45)	18.89 (15)	3.45 (8)	20.53 (18)	1.47 (3)	9.33 (9)	<DL	0.49 (3)	3.83 (8)	42.58 (44)	100.56	
	Spa (n=17)	<DL	<DL	<DL	<DL	88.37 (32)	4.17 (5)	0.90 (24)	0.031 (3)	0.22 (1)	93.69	0.0081 (8)
	Sul (n=5)	<DL	<DL	<DL	<DL	61.94 (17)	5.59 (53)	27.17 (254)	0.074 (25)	1.48 (27)	96.25	0.019 (6)
PR390	Sil (n=10)	20.27 (6)	1.53 (3)	19.01 (14)	1.69 (3)	9.37 (10)	<DL	0.16 (1)	5.17 (8)	41.48 (23)	98.69	
	Spa (n=16)	<DL	<DL	<DL	<DL	88.08 (17)	4.67 (16)	1.11 (19)	0.036 (9)	0.16 (1)	94.06	0.0070 (18)
	Sul (n=4)	<DL	<DL	<DL	<DL	62.82 (104)	6.49 (32)	27.26 (256)	0.045 (14)	0.62 (15)	97.24	0.009 (3)
PR394	Sil (n=33)	20.23 (4)	1.51 (2)	18.89 (8)	1.72 (2)	9.45 (6)	<DL	0.18 (1)	5.11 (5)	41.40 (15)	98.50	
	Spa (n=22)	<DL	<DL	<DL	<DL	86.84 (53)	5.20 (6)	1.10 (35)	0.049 (6)	0.20 (2)	93.38	0.0096 (11)
	Sul (n=5)	<DL	<DL	<DL	<DL	62.06 (67)	4.96 (233)	31.14 (250)	0.066 (44)	0.45 (8)	98.68	0.013 (9)
PR395	Sil (n=20)	19.83 (5)	1.40 (3)	19.01 (21)	1.65 (3)	10.66 (7)	<DL	0.26 (1)	4.66 (11)	41.21 (28)	98.67	
	Spa (n=9)	<DL	<DL	<DL	<DL	87.74 (46)	5.05 (12)	1.49 (27)	0.029 (7)	0.23 (4)	94.54	0.0063 (16)
	Sul (n=3)	<DL	<DL	<DL	<DL	63.33 (270)	7.52 (144)	26.13 (116)	0.051 (27)	0.55 (14)	97.59	0.011 (6)
PR377	Sil (n=47)	20.63 (15)	1.46 (13)	19.54 (26)	1.82 (19)	8.28 (15)	<DL	0.14 (4)	5.24 (40)	41.97 (71)	99.06	
	Spa (n=24)	<DL	<DL	<DL	<DL	84.07 (31)	5.00 (9)	6.65 (24)	0.038 (8)	0.16 (1)	95.93	0.0073 (17)
PR378	Sil (n=59)	20.62 (7)	1.54 (5)	19.59 (20)	1.81 (9)	8.55 (14)	<DL	0.38 (2)	5.68 (44)	42.48 (45)	100.68	
	Spa (n=15)	<DL	<DL	<DL	<DL	83.12 (61)	5.19 (11)	7.36 (51)	0.037 (10)	0.19 (1)	95.91	0.0065 (18)
PL191	Sil (n=21)	20.29 (7)	1.59 (3)	18.63 (14)	1.76 (3)	9.36 (10)	<DL	0.15 (1)	5.43 (10)	41.44 (27)	98.66	
	Spa (n=28)	<DL	<DL	<DL	<DL	83.06 (81)	5.61 (24)	7.18 (56)	0.036 (8)	0.18 (1)	96.06	0.0066 (14)
PR396	Sil (n=18)	20.26 (7)	1.64 (2)	18.29 (17)	1.78 (4)	9.45 (6)	<DL	0.13 (1)	5.34 (13)	41.22 (27)	98.11	
	Spa (n=9)	<DL	<DL	<DL	<DL	82.07 (36)	5.39 (12)	7.43 (27)	0.033 (7)	0.17 (1)	95.10	0.0062 (13)

Same abbreviations as in Table 1.

[a] Low alloy totals are probably due to the presence of C which was not analysed quantitatively.

[b] Number of electron microprobe analyses.

[c] Numbers in parentheses are 2 standard errors cited in term of least digits.

[d] Concentrations below the limit of detection of the electron microprobe are marked with the notation '<DL'.

S in the alloy increases the solubility of K in the alloy as suggested previously (e.g. [13,21,42]). It could also be related to variations of C and O contents in the two types of alloy. As shown in Fig. 4, if S had a direct influence on K partitioning, then D_K values should be higher at 7.7 GPa where the alloy contains ~7 wt.% S than at 1.0 and 3.6 GPa where the alloy contains ~1 wt.% S. However, we do not observe any gradual increase of D_K with S alloy content. Similarly, there is no well-defined correlation between D_K and C alloy content. Distinct D_K values are actually obtained for C alloy content between 4–5 wt.% depending on the type of alloy. From these observations, we conclude that neither S nor C alloy content is a major factor controlling K partitioning. Instead, we believe oxygen may play a major role. We found a broad positive correlation between D_K and D_O values from this study (Fig. 5a). When compared to the

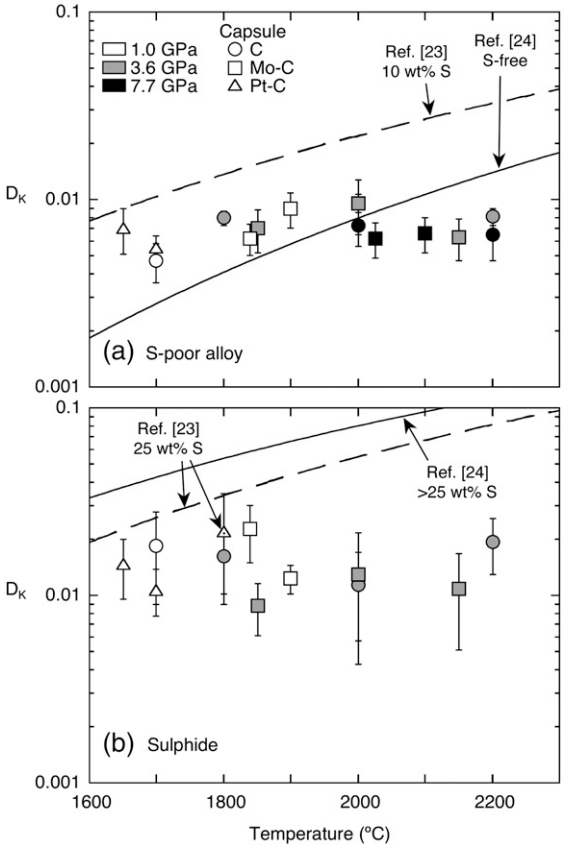

Fig. 3. Alloy–silicate partition coefficients for potassium (D_K) shown as a function of temperature. (a) Data for S-poor alloy and (b) data for sulphide. Dashed lines are predictions from Murthy et al. [23]. Solid lines are best fit to previously published experimental data from Bouhifd et al. [24] for S-free alloy and sulphide containing between 25 and 40 wt.% S). Our data for sulphide agree well with the experimental data point of Murthy et al. [23] at 2 GPa and 1800 °C. However, our results do not reveal any temperature dependence on K partitioning.

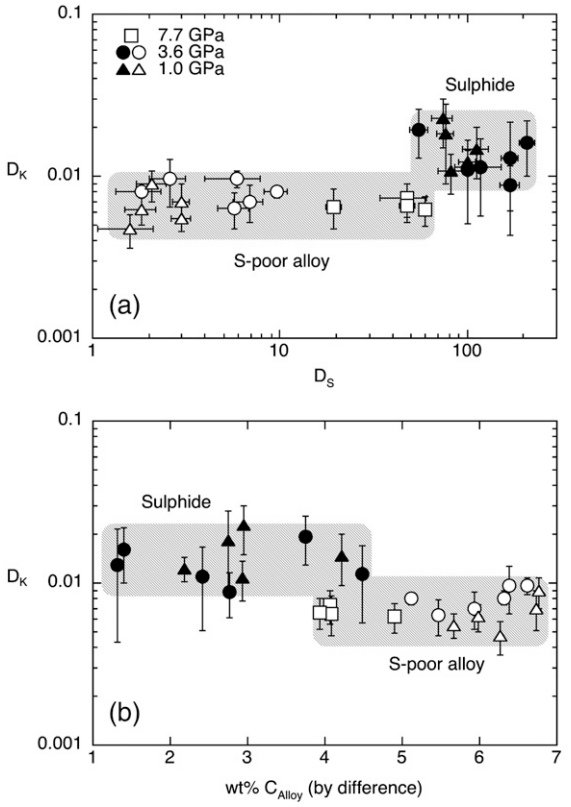

Fig. 4. Potassium partition coefficient shown as a function of (a) sulphur partition coefficient and (b) carbon alloy content (measured by difference). A correlation between these variables would be expected if sulphur and carbon alloy contents were predominant factors on K partitioning. We observe no systematic variation of D_K with D_S or C_{Alloy} suggesting that these elements do not control K partitioning.

results of Gessmann and Wood [22], the trend becomes unambiguous and suggests a potential dependence of D_K on D_O. Their sulphide–silicate partitioning data at oxygen fugacity near IW−2 are in good agreement with our results (Fig. 5b). Their data at more oxidized conditions (IW−1 to IW+1) extend the correlation obtained at IW−2 for sulphide and S-poor alloy to higher D_K–D_O values. Since the oxygen content of the silicate melt is approximately constant in our experiments and those of Gessmann and Wood [22] (~40–45 wt.%), this suggests that D_K may be controlled by O alloy content alone. The amount of potassium entering S–C–O–bearing core materials segregating through a magma ocean would depend primarily on the amount of oxygen incorporated in these core materials.

3.4. Potassium volatilization during experiment

One of the motivations of Murthy et al. [23] was to use double platinum–graphite capsules to avoid loss of

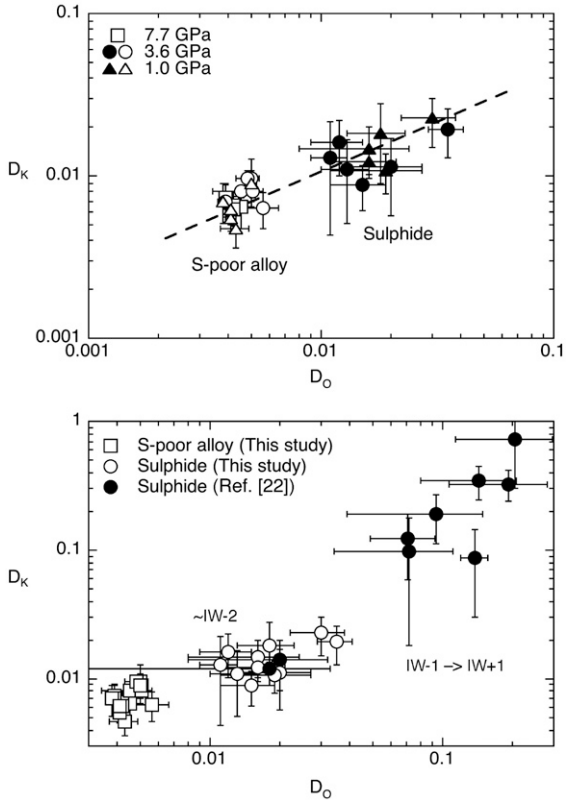

Fig. 5. Potassium partition coefficient plotted as a function of oxygen partition coefficient. The observed correlation between D_K and D_O and O_{Alloy} (since the oxygen content of the silicate melt is almost constant) suggests that O may have a significant effect on K partitioning between S-bearing liquid alloy and silicate melt. Data from Gessmann and Wood [22] agree with this interpretation.

potassium by volatilization during experiment. As shown in Table 1, K loss calculated by mass balance is 15±4% of the initial content (4.7 wt.%). If K loss affects preferentially one phase (alloy or silicate), partition coefficients derived from our experiments do not reflect true equilibrium between alloy and silicate. It is therefore important to evaluate the effect of K loss on partitioning. Some observations support the view that the experiments represent equilibrium conditions. First, experiments performed in sealed Pt–C also show some K loss (~15%). Since no K loss is expected from these experiments, it is likely that volatilization took place prior to the experimental runs, most probably during decarbonation of the starting material. Thus, we believe that all runs showing ~10–20% loss did not actually suffer any significant loss during the experiment, hence the corresponding partition coefficients reflect the equilibrium between alloy and silicate. This is the case for all runs except two runs using C-only capsules at 3.6 GPa (PR381, PR382) which have ~40% K loss (Table 1). Despite the important loss in these runs, however, D_K values are identical, within uncertainties, to the ones derived for runs PR394 and PR395, which were performed at similar conditions but which suffered less K loss (~20%). Therefore, we conclude that K volatilization during experimentation is unlikely to affect considerably K partitioning.

4. Conclusions

Our conclusions are:

(1) Partitioning of K between peridotitic melt and core-like Fe–Ni–S–C–O alloys is independent of temperature and pressure up to 2200 °C and 7.7 GPa.

(2) O, rather than S or C appears to affect K partitioning, with D_K increasing with increasing D_O. Therefore, the amount of K entering S–C–O–bearing core materials segregating in a magma ocean depends essentially on the amount of oxygen in the alloy. At present, it is not clear whether oxygen contributes significantly to the light element budget of the core. Volatility considerations [43] and melting phase relations in the Fe–(Mg,Fe)O system at high pressures [41,43–45] favour a small amount of O in the Earth's core. In contrast, mantle abundances of many moderately siderophile elements are more consistent with core formation under low oxygen fugacity conditions [46]. However, the effect of pressure on oxygen solubility in liquid alloys remains unresolved and controversial. A recent experimental study using a diamond anvil cell [47] found that oxygen solubility in metal alloys increases with increasing pressure, possibly because of low spin-high spin transition or metallization of FeO at megabar pressures [48,49]. Clearly, the question of the amount of oxygen in the core remains unanswered. Assuming no major effect of pressure and temperature on the correlation observed between D_O and D_K (Fig. 5b) and a K mantle content of ~240 ppm [7], a core containing S, C and ~2 wt.% O (i.e. D_O=0.05) would contain 2–25 ppm K (i.e. D_K=0.01–0.1). This amount corresponds to a present-day heat production of up to 0.2 TW, a small fraction compared to the estimated heat flux across the core-mantle boundary (~6–15 TW, e.g. [5]). If oxygen is the sole light element in the core, then ~9 wt.% would be sufficient to account for the density deficit [50]. However, since a combination of light elements is most likely [51,52], a more

reasonable upper limit for the oxygen content is on the order of 5 wt.%. Assuming an oxygen content of ~5 wt.% as suggested recently by Badro et al. [53] from seismic wave velocity measurements, core K content could be as high as ~80 ppm, which would produce slightly more heat (~0.5 TW).

5. Future work

In addition to constraining further the oxygen content of the core, there is a need to generate alloy–silicate partition coefficients for K at pressures above the putative electronic transition to resolve the issue discussed in this paper. Although analytically challenging, partitioning experiments in diamond–anvil cell or a modified multi-anvil press could be used to constrain the effect of pressure on K partitioning. The first of such experiments [54] have been reported, however, the lack of an elemental mass balance (their Table 1) between the run products and the starting material calls into question the reliability of interpretations of these results.

Acknowledgements

This manuscript benefited from discussions with Gudmundur Gudfinnsson, Valérie Malavergne, Rama Murthy, Bjorn Mysen, Mathieu Roskosz, Julien Siebert, Jon Wade, Heather Watson, Wim van Westrenen and Bernard Wood. We thank Chris Hadidiacos and Norman Pearson for technical assistance. Constructive reviews from John Lassiter and an anonymous reviewer and editorial comments from Richard Carlson are gratefully acknowledged. The Carnegie Institution of Washington (Postdoctoral Fellowships to AC and SK), the NASA (Cosmochemistry Grant NNG04GG09G to YF) and the NSF (Grant EAR0337621 to WFM) supported this work. Funding for the GEMOC electron microprobe comes from ARC LIEF and DEST Systemic Infrastructure Grants, Macquarie University and industry. This is contribution no. 455 from the ARC GEMOC National Key Centre (www.es.mq.edu.au/GEMOC/).

References

[1] D. Gubbins, T.G. Masters, J.A. Jacobs, Thermal evolution of the Earth's core, Geophys. J. R. Astron. Soc. 59 (1979) 57–99.
[2] B.A. Buffett, Estimates of heat flow in the deep mantle based on the power requirements for the geodynamo, Geophys. Res. Lett. 29 (2002), doi:10.1029/2001GL014649.
[3] B.A. Buffett, The thermal state of Earth core, Science 299 (2003) 1675–1677.
[4] S. Labrosse, Thermal and magnetic evolution of the Earth's core, Phys. Earth Planet. Inter. 140 (2003) 127–143.
[5] J.C. Lassiter, Constraints on the coupled thermal evolution of the Earth's core and mantle, the age of the inner core, and the origin of the $^{186}Os/^{188}Os$ "core signal" in plume-derived lavas, Earth Planet. Sci. Lett. 250 (2006) 306–317.
[6] U.R. Christensen, A. Tilgner, Power requirement of the geodynamo from ohmic losses in numerical and laboratory dynamos, Nature 429 (2004) 169–171.
[7] W.F. McDonough, S.-S. Sun, The composition of the Earth, Chem. Geol. 120 (1995) 223–253.
[8] K. Lodders, Solar system abundances and condensation temperatures of the elements, Astrophys. J. 591 (2003) 1220–1247.
[9] W.F. McDonough, The composition of the Earth, in: R. Teisseyre, E. Majewski (Eds.), Earthquake Thermodynamics and Phase Transformations in the Earth's Interior, Academic Press, San Diego, 2001, pp. 3–23.
[10] M. Humayun, R.N. Clayton, Potassium isotope cosmochemistry: genetic implications of volatile element depletion, Geochim. Cosmochim. Acta 59 (1995) 2131–2148.
[11] C.K. Gessmann, D.C. Rubie, The origin of the depletions of V, Cr and Mn in the mantles of the Earth and Moon, Earth Planet. Sci. Lett. 184 (2000) 95–107.
[12] N.L. Chabot, C.B. Agee, Core formation in the Earth and Moon: new experimental constraints from V, Cr, and Mn, Geochim. Cosmochim. Acta 67 (2003) 2077–2091.
[13] J.S. Lewis, Consequences of the presence of sulfur in the core of the Earth, Earth Planet. Sci. Lett. 11 (1971) 130–134.
[14] M.S.T. Bukowinski, The effect of pressure on the physics and chemistry of potassium, Geophys. Res. Lett. 3 (1976) 491–503.
[15] M. Somerville, T.J. Ahrens, Shock compression of $KFeS_2$ and the question of potassium in the core, J. Geophys. Res. 85 (1980) 7016–7024.
[16] D.M. Sherman, Chemical bonding and the incorporation of potassium into the Earth's core, Geophys. Res. Lett. 17 (1990) 693–696.
[17] L.J. Parker, T. Atou, J.V. Badding, Transition element-like chemistry for potassium under pressure, Science 273 (1996) 95–97.
[18] K.K.M. Lee, R. Jeanloz, High-pressure alloying of potassium and iron: radioactivity in the Earth's core? Geophys. Res. Lett. 30 (2003), doi:10.1029/2003GL018515.
[19] M.T. Murrell, D.S. Burnett, Partitioning of K, U and Th between sulphide and silicate liquids: implications for radioactive heating of planetary cores, J. Geophys. Res. 91 (1986) 8126–8136.
[20] E. Ito, K. Morooka, Dissolution of K in molten iron at high pressure and temperature, Geophys. Res. Lett. 20 (1993) 1651–1654.
[21] N.L. Chabot, M.J. Drake, Potassium solubility in metal: the effects of composition at 15 kbar and 1900 °C on partitioning between iron alloys and silicate melts, Earth Planet. Sci. Lett. 172 (1999) 323–335.
[22] C.K. Gessmann, B.J. Wood, Potassium in the Earth's core? Earth Planet. Sci. Lett. 200 (2002) 63–78.
[23] V.R. Murthy, W. Van Westrenen, Y. Fei, Experimental evidence that potassium is a substantial radioactive heat source in planetary cores, Nature 423 (2003) 163–165.
[24] M.A. Bouhifd, L. Gautron, N. Bolfan-Casanova, V. Malavergne, T. Hammouda, D. Andrault, A.P. Jephcoat, Potassium partitioning into molten iron alloys at high-pressure: implications for Earth's core, Phys. Earth Planet. Inter. 160 (2007) 22–33.
[25] J. Li, C.B. Agee, Geochemistry of mantle-core differentiation at high pressure, Nature 381 (1996) 686–689.

[26] K. Righter, M.J. Drake, Metal-silicate equilibrium in a homogeneously accreting earth: new results for Re, Earth Planet. Sci. Lett. 146 (1997) 541–553.
[27] J. Li, C.B. Agee, The effect of pressure, temperature, oxygen fugacity and composition on partitioning of nickel and cobalt between liquid Fe–Ni–S alloy and liquid silicate: implications for the earth's core formation, Geochim. Cosmochim. Acta 65 (2001) 1821–1832.
[28] D.C. Rubie, H.J. Melosh, J.E. Reid, C. Liebske, K. Righter, Mechanisms of metal–silicate equilibration in the terrestrial magma ocean, Earth Planet. Sci. Lett. 205 (2003) 239–255.
[29] G. Dreibus, H. Palme, Cosmochemical constraints on the sulfur content in the Earth's core, Geochim. Cosmochim. Acta 60 (1996) 1125–1130.
[30] C. Allègre, G. Manhès, E. Lewin, Chemical composition of the Earth and the volatility control on planetary genetics, Earth Planet. Sci. Lett. 185 (2001) 49–69.
[31] Y. Thibault, M.J. Walter, The influence of pressure and temperature on the metal–silicate partition coefficients of nickel and cobalt in a model C1 chondrite and implications for metal segregation in a deep magma ocean, Geochim. Cosmochim. Acta 59 (1995) 991–1002.
[32] J.T. Wasson, G.W. Kallemeyn, Compositions of Chondrites, Philos. Trans. R. Soc. Lond., A 325 (1988) 535–544.
[33] W. Van Westrenen, J.A. Van Orman, H. Watson, Y. Fei, E.B. Watson, Assessment of temperature gradients in multianvil assemblies using spinel layer growth kinetics, Geochem. Geophys. Geosys. 4 (2003), doi:10.1029/2002GC000474.
[34] S.R. Bohlen, A.L. Boettcher, The quartz–coesite transformation: a precise determination and the effects of other components, J. Geophys. Res. 87 (1982) 7073–7078.
[35] T. Yagi, M. Akaogi, O. Shimomura, T. Suzuki, S. Akimoto, In situ observation of the olivine–spinel phase transformation in Fe_2SiO_4 using synchrotron radiation, J. Geophys. Res. 92 (1987) 6207–6213.
[36] J. Susaki, M. Akaogi, S. Akimoto, O. Shimomura, Garnet–perovskite transition in $CaGeO_3$: in-situ X-ray measurements using synchrotron radiation, Geophys. Res. Lett. 12 (1985) 729–732.
[37] J. Zhang, B. Li, W. Utsumi, R.C. Liebermann, In situ X-ray observations of the coesite–stishovite transition: reversed phase boundary and kinetics, Phys. Chem. Miner. 23 (1996) 1–10.
[38] S. Urakawa, M. Kato, N. Takahashi, T. Katsura, Closure of liquid immiscibility gap in the system Fe–C–S at high pressure, EOS Trans. AGU 86 (2005) (Abstract MR13A–0075).
[39] K. Tsuno, E. Ohtani, H. Terasaki, Phase relations in the Fe–O–S system at high pressures, EOS Trans. AGU 86 (2005) (Abstract MR13A–0058).
[40] J. Li, C.B. Agee, Element partitioning constraints on the light element composition of the Earth's core, Geophys. Res. Lett. 28 (2001) 81–84.
[41] D.C. Rubie, C.K. Gessmann, D.J. Frost, Partitioning of oxygen during core formation on the Earth and Mars, Nature 429 (2004) 58–61.
[42] H.T. Hall, V.R. Murthy, The early chemical history of the Earth: some critical elemental fractionations, Earth Planet. Sci. Lett. 11 (1971) 239–244.
[43] H.S. O'Neill, D. Canil, D.C. Rubie, Oxide-metal equilibria to 2500 °C and 25 GPa: implications for core formation and the light component in the Earth's core, J. Geophys. Res. 103 (1998) 12239–12260.
[44] A.E. Ringwood, W. Hibberson, The system Fe–FeO revisited, Phys. Chem. Miner. 17 (1990) 313–319.
[45] R. Boehler, Melting of the Fe–FeO and the Fe–FeS systems at high pressure: constraints on core temperatures, Earth Planet. Sci. Lett. 111 (1992) 217–227.
[46] J. Wade, B.J. Wood, Core formation and the oxidation state of the Earth, Earth Planet. Sci. Lett. 236 (2005) 78–95.
[47] N. Takafuji, K. Hirose, N. Mitome, Y. Bando, Solubilities of O and Si in liquid iron in equilibrium with $(Mg,Fe)SiO_3$ perovskite and the light elements in the core, Geophys. Res. Lett. 32 (2005), doi:10.1029/2005GL022773.
[48] E. Knittle, R. Jeanloz, High-pressure metallization of FeO and implications for the Earth's core, Geophys. Res. Lett. 13 (1986) 1541–1544.
[49] J. Badro, V.V. Struzhkin, J. Shu, R.J. Hemley, H.K. Mao, J.-P. Rueff, C.C. Kao, G. Sheu, Magnetism in FeO at megabar pressures from X-ray emission spectroscopy, Phys. Rev. Lett. 83 (1999) 4101–4104.
[50] J.-P. Poirier, Light elements in the Earth's outer core: a critical review, Phys. Earth Planet. Inter. 85 (1994) 319–337.
[51] V.J. Hillgren, C.K. Gessmann, J. Li, An experimental perspective on the light element in Earth's core, in: R.M. Canup, K. Righter (Eds.), Origin of the Earth and Moon, University of Arizona Press, Tucson, 2000, pp. 245–263.
[52] W.F. McDonough, Compositional model for the Earth's core, in: R.W. Carlson (Ed.), Treatise on Geochemistry the Mantle and Core, vol. 2, Elsevier-Pergamon, Oxford, 2003.
[53] J. Badro, G. Fiquet, F. Guyot, E. Gregoryanz, F. Occelli, D. Antonangeli, M. d'Astuto, Effect of light elements on the sound velocities in solid iron: implications for the composition of Earth's core, Earth Planet. Sci. Lett. 254 (2007) 233–238.
[54] N. Hirao, E. Ohtani, T. Kondo, N. Endo, T. Kuba, T. Suzuki, T. Kikegawa, Partitioning of potassium between iron and silicate at the core–mantle boundary, Geophys. Res. Lett. 33 (2006).